

MODELING THE IMPACT OF UNCERTAINTY IN DETECTOR SPECIFICATION ON EFFICIENCY VALUES OF A HPGe DETECTOR USING ANGLE SOFTWARE

by

Maurice MILLER* and Mitko VOUTCHKOV

Department of Physics, University of West Indies, Mona, Jamaica

Scientific paper

DOI: 10.2298/NTRP1302169M

The objective of this study is to model the impact of uncertainties in the engineering specifications of a typical p-type HPGe detector on the efficiency values when the measured soil sample is in contact geometry with the detector. We introduce a parameter named the normalized sensitivity impact which allows a comparative analysis to be made of the impact of the detector specification uncertainties and develop a correction factor table for the most important parameters. The areas of the detector most susceptible to error were found to be the crystal geometry, vacuum layer above the crystal and the bulletizing radius. In all cases the major impacts were mathematically modeled – for the first time – and found to vary either quadratically or logarithmically over the energy range of 180 keV to 1500 keV. Finally, we propose a set of detector characterization values that may be used in ANGLE for generating a reference efficiency curve using the efficiency transfer method inherent in this software. These values are to be used with the understanding that their uncertainty impact on the full-peak efficiency though not very significant in this counting arrangement, is not non-zero.

Key words: detector characterization, ANGLE, uncertainty, HPGe, detector efficiency

INTRODUCTION

The engineering designs of typical HPGe radiation detectors include specifications that characterize them such as crystal height and length, vacuum top and side thickness, bulletizing radius, core geometry, inactive top and side layer thickness, contact material, contact pin material, contact pin radius, end-cap window and material, and detector housing. When these numerous parameters are incorrectly entered or contain errors in their measurement, systematic errors will be introduced in gamma activity measurements when using absolute Monte Carlo (MC) or semi-empirical models such as ANGLE software. A typical detector set-up in a semi-empirical model may require as much as 70 parameters with Monte Carlo methods requiring much more detailed specification. Invariably, the spectrometrists may encounter significant challenges in accessing the technical specifications from the manufacturer, and cases have been known where the specification sent contained errors. Transcription errors entering these many parameters cannot be overlooked as some of the inputs are values well below unity.

Until now, not much can be said about where the highest level of sensitivity to error lies in an HPGe de-

tor designed for the radiometric analysis of soil and sediment samples in contact geometry with the detector. For this study, we limited our investigation to a cylindrical source in contact geometry with a p-type 180 cm³ closed-end coaxial HPGe detector fully enclosed in a lead container to reduce terrestrial and cosmic radiation. This is a popular geometry for counting gammas from soil or beach sediment samples. The gammas of interest are those of primordial origin such as the actinium, uranium, and thorium series in the range of 180 keV-1500 keV, and the non-series K-40 at 1460 keV. We have not considered Marinelli sources and the other types of semi-conductor detectors such as n-types, well-type or semi-planar low-energy photon detectors (LEPD), or multiple crystal sizes found in detectors used in soil gamma spectrometry. These may be investigated in a further study.

While other factors outside of the detector can impact one's ability to accurately determine the analysis of the radioisotopes of interest, our investigation will be limited to the engineering specification of the typical HPGe detector used for environmental analysis of soil and sediment samples. Specifically we seek to determine quantitatively, how errors in the various components of the engineering design impact the efficiency or reported radioactivity measurements. With a knowledge of the error sensitivity of the key compo-

* Corresponding author; e-mail: moneilmiller@gmail.com

nents, spectrometrists using MC or semi-empirical methods will now be able to focus more on specific engineering parameters to ensure that systematic errors are minimized in the measurement process.

Numerous investigations into uncertainties in various aspects of the nuclear instrumentation processes covering photomultiplier detector, detector dead time, decay data due to coincidence summing, measurements in CR-39 track detectors, uncertainty bound to radon progeny equilibrium factors, energy loss in silicon, Sr-90 concentrations in powder samples, and in-situ gamma spectrometry measurements of air cleaning filters have been published [1-12]. These works highlight the importance of modeling uncertainties in the nuclear measurement process in order to reduce systematic errors and produce results that can sustain scientific scrutiny and experimental reproducibility. In addition, parametric studies of uncertainty propagation in CANDU reactor to quantify the uncertainty in the detector layout using as much as 343 sets of uncertainty values to produce corresponding trip set points in the reactor have been done [13]. Unfortunately, not much work has been published dealing with error propagation in HPGe detectors setup specifically for measuring soil radioactivity. A very comprehensive publication by Mihaljevic *et al.* dealing with the effect of ignoring bulletization in various detector-source geometries represents the closest study to this work. Their paper applied a mathematical treatment to disc, cylindrical and Marinelli sources in various geometries with n-type, p-type HPGe, thick LEPD detectors, simulating the impact of various bulletizing radius. The detectors used in their simulation covered variations in crystal radius, crystal height, dead layer, core height, core radius, contact thickness, crystal to end-cap distance, end cap thickness, and window thickness. They concluded that bulletizing radius error can lead to considerable systematic errors (tens of percent's) especially for low gamma energies and close counting arrangements [14]. Regarding the effect of bulletizing radius, this paper examined the impact of assuming a common 8 mm bulletizing radius when in fact the detector had no bulletizing radius. In the discussion section of this paper we identified areas of commonality in these two papers and explained how the existing theory of gamma detection supports the results we propose. We note that the purpose of bulletization is primarily for eliminating the weak electric fields found at the edges of the cylindrical detector crystal [15]. However, there is no universal consensus here, as Princeton Gamma-Tech (PGT) surmises that the variation in the electric field that is avoided by this design is minor and so they do not manufacture crystals with bulletizing radius [16].

The production of the absolute efficiency curve for a particular detector is one of the most important functions in radiometric analysis. Using the experimen-

tal approach, the efficiency curve must however be generated by a reference standard for each geometry that will be encountered. Invariably, the reference standard may not be available in all the geometries required. In order to overcome this challenge, spectrometrists may use absolute methods such as Monte Carlo or semi-empirical methods such as ANGLE to generate a reference efficiency curve for a specified geometry using available reference standards in a particular geometry. For example in this study, we used the efficiency transfer function of ANGLE to convert the efficiency curve of disc source counted 25 cm above the detector to that for a cylindrical source in contact geometry. The experimental curve for the source in contact geometry was compared to the ANGLE simulated curve for the similar geometry and used for quality assurance for the simulated results presented in this paper. In general, the error variation in the efficiency curves may be attributable to error introduced in the experimental measurement process and poor detector specification, especially for the active body, inactive layers, vacuum and compositional details of all elements in the source and detector [17]. The detector's characteristics may also contribute to errors since some gammas may have been scattered and absorbed in the detector's end-cap window and in the Ge inactive or dead layer. Additionally some gammas may not have produced a signal inside the detector's active volume if their energy is lower than the detector's discriminator threshold. For gamma energies up to 40 keV, the relationship between energy and efficiency is strongly affected by the attenuation of these photons by materials outside the detector, such as the intercepting layers, and the dead layer surrounding the detector. Detector manufacturers have made engineering interventions to reduce this attenuation of the low energies. Ortec reports that its gamma-X n-type detectors allow photons with energies as low as 3 keV to enter the detector's active volume as a result of the 0.3 m boron ion-implanted contact and thin beryllium front window. For the measurement of primordial gamma radiation in soils, we are rarely concerned with energies in the vicinity of 40 keV and below. Most likely the gammas of interest in the lower energies are the U-235 peaks at 144, 163, and 185 keV and the Th-234 peak at 63 keV. The U-235 peak at 185.71 keV may be very problematic to isolate due to its overlap with Ra-226 at 186.21 keV.

ANGLE is an application running in a Windows based environment that calculates full energy peak efficiencies for a variety of detectors such as HPGe true and closed-end coaxial, Ge(Li) open and closed-end, planar low energy photon detectors (LEPD) and well-type detectors. ANGLE uses the effective solid angle concept and supports cylindrical or Marinelli sources for coaxial positioning; samples may also be point, disc, or bulky samples. ANGLE's use has been reported in many publications. A detailed description of ANGLE has been published by its developer [17].

Efficiency calibrations comparisons between ANGLE and LabSOSCS have found deviations within 10% in experimental versus calculated efficiency calibrations for three HPGe detectors [18]. Many other studies involving the use of ANGLE have been published [17, 19-24].

SUMMARY OF THE THEORETICAL

ANGLE uses the concept of the effective solid angle ($\bar{\Omega}$) to calculate the value of the energy dependent full-energy peak efficiency or absolute efficiency qualitatively defined in eq. (1)

$$\epsilon_{\text{abs}} = \frac{\text{number of pulses recorded in detector}}{\text{number of radiation quanta emitted by source}} \quad (1)$$

This efficiency is impacted by the detector properties and the solid angle ($\bar{\Omega}$) subtended by the radioactive source counted on the face of the detector. The absolute efficiency of the sample ϵ_{abs} is related to that of the reference standard $\epsilon_{\text{abs,ref}}$ by the expression in eq. (2) [25]

$$\epsilon_{\text{abs}} = \epsilon_{\text{abs,ref}} \frac{\bar{\Omega}}{\bar{\Omega}_{\text{ref}}} \quad (2)$$

Assuming a gamma source (S) and detector (D) shown in fig. 1, the effective solid angle may be defined as shown in eqs. (3) and (4), where S_D is the surface of the detector exposed to the gamma photons and V_s is the volume of the source, T is a point varying over V_s , P is a point varying over S_D , and n_u is the external unit vector normal to an infinitesimal area $d\sigma$ on S_D . F_{att} accounts for the gamma attenuation that occurs

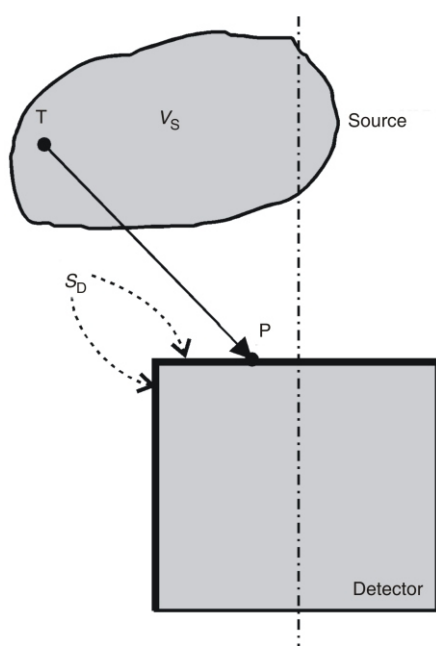


Figure 1. Defining the solid angle [26]

when the photon emerges from the detector volume in the direction TP . F_{eff} relates to the probability of a photon, degraded in energy, interacting within the detector active volume

$$\bar{\Omega} = \int_{V_s, S_D} d\bar{\Omega} \quad (3)$$

and

$$d\bar{\Omega} = \frac{F_{\text{att}} F_{\text{eff}} TP n_u d\sigma}{|TP|^3} \quad (4)$$

In the case where the source is a cylindrical source positioned above the detector, as shown in fig. 2, the solid angle ($\bar{\Omega}$) for the above geometry where $r_0 < R_0$ may be expressed as shown in eq. (5)

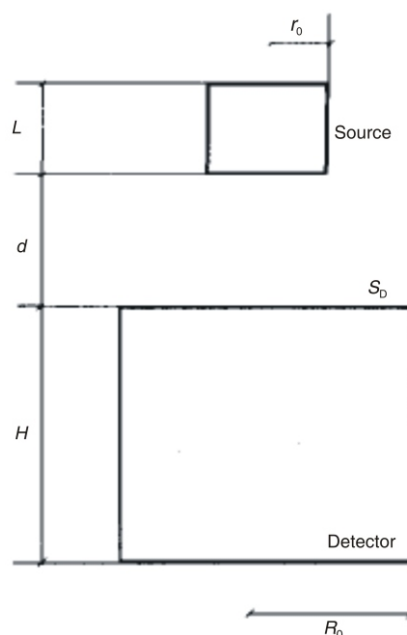


Figure 2. Cylindrical source above detector, for solid angle development

$$\bar{\Omega} = \frac{4}{r_0^2 L} \int_0^L \int_0^{r_e} \int_0^\pi \frac{F_{\text{att}} F_{\text{eff}} R dR}{[R^2 - 2R \cos \phi + r^2 + (d-l)^2]^{3/2}} r dr d\phi \quad (5)$$

where

$$\phi = \arctg \sqrt{\frac{r^2 + R_0^2}{R_0}}$$

Cases where $r_0 > R_0$ for the above geometry and Marinelli sources, have been adequately covered by Mihaljević *et al.* They have also shown that when detector bulletizing radius is being considered (as in this paper) the solid angle may be expressed as shown in eq. (6). Further details are provided for sources whose radii exceed that of the detector, $r_0 > R_0$. For the counting arrangement encountered in this paper, $r_0 < R_0$ [17]

$$\bar{\Omega} = \int_{(V_1, V_2), S_1} \int_{V_2, S_2} d\bar{\Omega} \quad (6)$$

Detector full-energy efficiency curves form the foundation on which accurate radioactivity is measured in environmental samples such as top soil using a standard and verifiable source counted above the detector. The specific activity (A) of the sample is measured by the formula

$$A(\gamma) = \frac{CPS}{\varepsilon(\gamma)mI_\gamma} \quad (7)$$

where CPS is the net count per second under the gamma peak of interest, I – the branching ratio, m – the mass, and $\varepsilon(\gamma)$ – the absolute or full energy peak efficiency for a particular gamma energy of interest. From eq. (7), it is apparent that any over-statement or under-statement of the efficiency value leads to an under-statement or over-statement, respectively, of the radioactivity of the sample.

The key is the determination of ε , which may be experimentally determined by fitting a function of the form shown in eq. (8) to a plot of full-energy efficiency versus gamma energies using a reference source of verifiable activity and reference date, to account for activity on the date of measurement. Various software can be used to determine the efficiency fitting parameters a , b , c , and d below, which can then be extrapolated to determine the gamma energies of interest. SigmaPlot version 10 was used in this research due to its ease of use and flexibility.

$$\varepsilon = \frac{aE^b}{1000 c E^d} \quad (8)$$

The absolute efficiency ε_{abs} is a function of the solid angle Ω ; the solid angle is dependent on the source to detector distance or counting geometry. In this paper, the geometry employed was with Eu 152/154 cylindrical and disc calibration sources; the former in contact geometry with the detector and the latter counted 25 cm above the face of the detector. Coincidence summing in gamma spectrometry, primarily due to complex decay schemes, close geometry, and where lifetimes of nuclear levels are much shorter than the charge collection time in detectors, impact the efficiency measurements. Summing corrections from a few percent to higher (few 10% for low-level measurements in Marinelli containers or well-type detectors) are sometimes required. Treatment of summation effects including continuum reduction and the Compton spectrometer method have been detailed [27].

MATERIALS AND METHODS

Overview

The results for this experiment were generated by the following three step method (a) two experimental reference efficiency (REC) curves were generated, one for a Eu-152 disc source positioned 25 cm above the

detector and counted for 1800 s and a cylindrical source (soil geometry) in contact geometry with the detector counted for 3600 s. (b) Information from Ortec on the technical specifications of the detector were input into ANGLE, and the experimental disc source's REC was used to generate the soil geometry's absolute efficiency curve (AEC). A comparison of both the experimental soil AEC and the simulated soil AEC was done for the contact geometry. This was used as a quality assurance method to validate the configuration of the detector in ANGLE simulation and justify using it to generate the data that were simulated. (c) The final procedure was to examine how erroneous measurements relating to the detector's crystal, core, vacuum, housing, dead layer, end-cap and end-cap window, contacts, compositional materials and detector housing were propagated to the AEC of the soil geometry. Incorrect detector parameter values were entered and the results of the new efficiency curves are compared with the correct efficiency curve to determine the percentage deviation. The values entered are shown in tab. 2 where the plus and minus integers indicate the variation from the true detector values. In some cases the values are halved or doubled, and where applicable construction materials are changed. In all instances, a Gauss coefficient of order 42 was used to generate the simulated data in ANGLE. ANGLE completed these calculations in less than a minute.

The experimental set-up was in keeping with geometry recommendation from the manufacturer Ortec regarding measurements for on end-cap samples such as ours, *i. e.*, that the detector's diameter should ideally exceed the sample diameter by at least 20% and that beyond 30% the gain in efficiency is negligible. If the detector diameter exceeds the sample by 20% or more then error due to irreproducibility of sample position will be minimal. The detector was fitted with a low-background carbon 0.76 mm fiber window, which resulted in a lower minimum detectable activity (MDA) for a specific counting time (Ortec 2011). In this set-up, the detector crystal diameter was 85 mm and the cylindrical calibration source container's diameter was 70 mm indicating that the detector was approximately 21.4% larger than the container. We were therefore satisfied that we are operating at optimum efficiency for the size of the container. A container with a larger diameter is therefore not only unnecessary but would only introduce errors due to geometry irreproducibility.

All analytical work was done using ANGLE version 3, SPECTRW, Datafit 9.0, SigmaPlot 10.0, \$RSUMUP, ENERCOR, Microsoft Excel and a customized file for correcting summing effects introduced by soil sample and calibration sources in contact geometry with this specific HPGe detector.

Experimental set-up

The generation of the experimental efficiency curves was carried using the Ortec GEM-FX8530P4 with a warranted resolution (FWHM) at 1.33 MeV (Co-60)=1.9 keV and factory reported measured value

of 1.76 keV. The amplifier shaping time was 6 ns, peak-to-Compton ratio (Co-60) was 55:1 (warranted) and 61:1 measured, relative efficiency at 1.33 MeV (Co-60) was 40.5%. The set-up consisted of a high voltage filter, detector, and pre-amplifier which were all housed in the detector lead housing. A recommended high voltage of 4800 V was applied to the detector from a FAST NHQ-205M NIM module [28]. The dimensions of the cylindrical container used for the soil and EU-152/154 efficiency measurements was as follows: diameter = 70 mm, height = 21 mm, bottom thickness = 1 mm, and side thickness = 1 mm. Details of the preparation of the Eu-152/154 calibration sources used in this paper have been published [29].

Detector parameters

Figure 3 shows the detector's configuration as supplied by the manufacturer, ORTEC. In ANGLE, the input data are categorized as detector, container, geometry, source and reference efficiency curve. The majority of the data requirement is for the detector. Details of the input to ANGLE are shown further in tab. 2.

Quality assurance

The experimental efficiency curve for both the disc and cylindrical Eu-152/154 sources were deduced from spectra analyzed in the SPECTRW V37-27 software. The disc source efficiency data was input to ANGLE 3 and used to generate an efficiency curve for a cylindrical geometry similar to the soil container. The ANGLE efficiency values were then compared to the experimental values for the gamma energies of interest in soil samples for the range 180 keV-1500 keV. Error values within 4% (of the experimental values) were obtained and are considered acceptable [17]. Figure 4 shows both the experimental

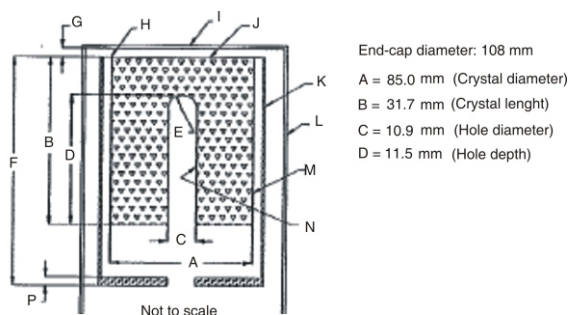


Figure 3. Detector parameters for GEM-FX8530P4 HPGC detector. Data courtesy of Ortec [30]
 E: Nominal 5 mm radius, F: 58 mm cup length, G: 5 mm space, H: 0.03 mm/0.03 mm Al/Mylar, I: 0.09 mm carbon fiber, J: <0.015 mm Ge/Li/ dead, K: 2.5 mm Al, L: 1 mm Al, M: 0.7 mm Ge/Li dead layer, N: 0.3 micron Ge/B dead layer, and P: 11 mm

Table 1. Percentage variation between experimental and ANGLE for absolute efficiency

Energies	Experimental full-peak efficiency values	ANGLE full-peak efficiency values	Percentage variation between ANGLE and experimental [%]
186.1	0.077228141	0.07716939	-0.08
238.63	0.061638994	0.06188052	0.39
241	0.061088997	0.06131016	0.36
241.91	0.060880547	0.06109351	0.35
295.2	0.050823094	0.0504024	-0.83
338.322	0.044911334	0.04406982	-1.87
351.4	0.043392708	0.04244894	-2.17
510.8	0.030908619	0.02966513	-4.02
582.7	0.027428747	0.02643554	-3.62
609.312	0.026339981	0.02547244	-3.29
661.66	0.024442755	0.02386221	-2.38
727.264	0.022434288	0.02224391	-0.85
910.8	0.018292488	0.01788789	-2.21
964.64	0.01736404	0.01691765	-2.57
968.971	0.017293633	0.01684415	-2.60
1120.4	0.015159689	0.01435839	-5.29
1460.83	0.011917432	0.0115639	-2.97

and the ANGLE-generated efficiency curves; tab. 1 shows the difference between the two curves over the region of 180 keV-1500 keV and the variation within the spectrum quantified in tab. 1. The gamma energies are those of the primordial radionuclides commonly found in uncontaminated soil samples.

RESULTS AND DISCUSSION

Summary of results

In this section we report on how the detector uncertainties investigated in tab. 2 propagated to the mean absolute/full-peak efficiency values over the range 180 keV-1500 keV. We introduce a normalized sensitivity impact (NSI) value which indicates the percentage change in the absolute efficiency values for each corresponding percent error introduced in the design parameter and defined as follows

$$NSI = \frac{\overline{\Delta \epsilon}}{|E|} \quad (9)$$

where $\overline{\Delta \epsilon}$ denotes the mean percentage change in absolute efficiency over the gamma range of 180 keV-1500 keV and $|E|$ = absolute value of percentage variation between true and error generated efficiency values. Another way of looking at the NSI parameter is that the percentage output error is normalized to the input error.

We concluded that the areas of highest sensitivity in the detector, shown in fig. 5, were the vacuum top thickness (NSI = 0.12), the crystal's radius (NSI = 0.55) and crystal height (NSI = 0.16). The detector bulletizing radius was shown to have an impact of +2.24% changes on the mean efficiency value when an

Table 2. Results of detector parameters investigated

ANGLE description	Error modeling description	Key	Correct value [mm]	Incorrect value [mm]	Input error [%]	Mean impact on efficiency [%]	Normalized sensitivity impact on absolute efficiency
Vacuum	Vacuum top thickness - 2 mm	Vtt - 2 mm	5	3	-40	4.76	0.12
Vacuum	Vacuum top thickness + 2 mm	Vtt + 2 mm	5	7	40	-4.34	-0.11
Vacuum	Vacuum side thickness - 2 mm	Vst - 2 mm	8	6	-25	0.04	0.00
Vacuum	Vacuum side thickness + 2 mm	Vst + 2 mm	8	10	25	0.04	0.00
Detector	Crystal radius - 2 mm	Dcr - 2 mm	42.5	4.05	-5	2.61	0.55
Detector	Crystal radius + 2 mm	Dcr + 2 mm	42.5	44.5	5	-2.62	-0.56
Detector	Crystal radius + 2 mm	Dch + 2 mm	31.7	29.7	-6	-0.98	-0.16
Detector	Crystal radius - 2 mm	Dch - 2 mm	31.7	33.7	6	0.04	0.01
Detector	Bulletizing radius	Dbr	0	8	n/a	2.24	n/a
Detector	Inactive Ge side thickness doubled	Igest-X2	0.7	1.4	100	0.96	0.01
Detector	Inactive Ge side thickness halved	Igest-h	0.7	0.35	-50	-0.42	-0.01
Detector	Inactive Ge top thickness doubled	Igett-X2	0.0015	0.003	100	-0.05	0.00
Detector	Inactive Ge top thickness halved	Igett-h	0.0015	0.00075	-50	0.02	0.00
End-cap window	End-cap window thickness halved	Ewt-h	0.9	0.45	-50	0.24	0.00
End-cap window	End-cap window material change	Ewm-c	Carbon fiber	Beryllium	n/a	0.08	n/a
End-cap	End-cap top thickness doubled	Ett-X2	1	2	100	-2.19	-0.02
End-cap	End-cap side thickness doubled	Est-X2	1	2	100	0.04	0.00
Detector	Core height + 2 mm	Dcorh + 2 mm	11.5	13.5	17	0.01	0.00
Detector	Core height - 2 mm	Dcorh - 2 mm	11.5	9.5	-17	-0.01	0.00
Detector	Core radius - 2 mm	Dcor - 2 mm	5.45	3.45	-37	-0.03	0.00
Detector	Core radius + 2 mm	Dcor + 2 mm	5.45	7.45	37	0.04	0.00
Detector	Change in contact material	Dcm - c	Ge with lithium ions	Aluminum	n/a	0.04	n/a
Detector	Change in contact pin material	Dcpm - c	Brass	Copper	n/a	0.04	n/a
Detector	Contact pin radius - 2 mm	Dcpr - 2 mm	3.175	1.175	-63	0.04	0.00
Detector	Contact pin radius + 2 mm	Dcpr + 2 mm	3.175	5.175	63	0.04	0.00
Detector	Contact side thickness doubled	DcstX2	0.003	0.006	100	0.04	0.00
Detector	Contact side thickness halved	Dcst-h	0.003	0.0015	-50	0.04	0.00
Housing	Inner side thickness - 2 mm	Hist - 2 mm	2.5	0.5	-80	0.04	0.00
Housing	Inner side thickness + 2 mm	Hist + 2 mm	2.5	4.5	80	0.04	0.00

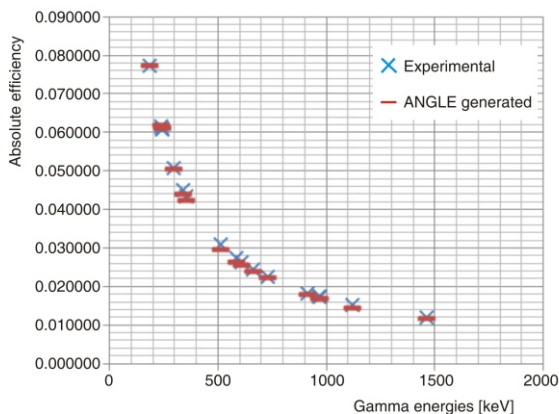


Figure 4. Experimental and simulated reference efficiency curves

incorrect value of 8 mm was assumed, the correct value being zero. The details of how these errors propagated at the various sections in the gamma energy

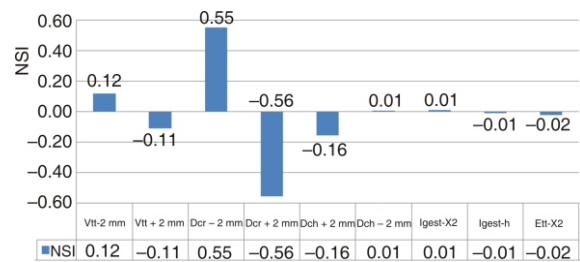


Figure 5. Summarizes the normalized sensitivity impact (NSI > 0.00) for the detector and geometry investigated in this report

spectrum are discussed further on in this paper. We also investigated the impact of changes in construction materials such as the contact material and the contact pin material, but their impact was deemed negligible for this counting geometry. Other components, where NSI = 0.00 as shown in tab. 2, appeared to be not very

significant areas of uncertainty for the counting arrangement investigated.

In the next subsections, we modeled the variation of the absolute efficiency curve (generated by the errors introduced) from the original and valid curve. The fitted functions describing the variations and their R-squared values are also presented. In the eqs. 11-16, x denotes the gamma energies in keV, and Y denotes the percentage change in the absolute efficiency value when the error is introduced.

Discussion for general results

Components with NSI = 0.00 as shown in tab. 2, appeared to be not very significant areas of uncertainty for this counting arrangement when investigating the gamma activity of soil samples. We conclude that the values in tab. 2 may be used as default values for similar detector-source set-up when the values are not readily available from their manufacturer and/or a preliminary efficiency curve is required. The zero NSI values for the contact material, contact pin radius, and pin material are not surprising since they do not directly affect the gamma solid angle hence photon interaction is in the active volume of the detector. The contact material for this detector was Ge with lithium ions which was modeled as a material with density of 5.323 g/cm³, Ge having a mass attenuation coefficient of 5.727E-02. The contact pin was simulated as comprising 60% copper, 39.25% zinc, and the remaining 0.75% being silicon; the density is assumed to be 8.41 g/cm³. Note these NSI values are not zero, but are rounded to two significant figures, so errors here do propagate to the efficiency value of the detector.

Table 3 is a set of correction values to be used to multiply the activity when trying to account for

uncertainties in the various parameters shown in the table. The correcting value C is derived from the expression

$$C_v = 1 + \frac{Y}{100} \quad (10)$$

Application of correcting function table

Assume the specific activity of Pb-214 at 295 keV was measured at 93.91 Bq/kg using efficiency values from ANGLE. If we wish to account for the range of values taking detector crystal radius error into consideration then the range of values for this specific activity value would be 93.91 0.972 to 93.91 1.028 or 93.91 ± 2.63 Bq/kg. Details of the derivation of the Y -value used in the correction function are shown in the following section.

Modeling of errors in detector vacuum geometry – top and side thickness

In this section we introduced two error scenarios into the efficiency calculation by changing the detector vacuum top thickness value of 5 mm to 3 mm and 7 mm. The resulting efficiency curves from these two scenarios were compared with the actual efficiency curve, and the average percentage value of the changes noted.

The vacuum top thickness value (in fig. 6 with arrow depiction) had an increase of 4.76% on the mean efficiency curve over the region of 180 keV-1500 keV, when the top thickness was under measured by 2 mm; a decline of 4.34% on the mean absolute efficiency values over the 180 keV-1500 keV range was noted when the same parameter was over measured by 2 mm. These er-

Table 3. Correcting values for various detector parameters

Gamma source	Gamma energy	Detector bulletizing radius	Crystal height – 2 mm	Crystal height + 2 mm	Crystal radius – 2 mm	Crystal radius + 2 mm	End-cap top thickness doubled	End-cap window thickness halved	Vacuum top thickness + 2 mm	Vacuum top thickness – 2 mm
U-235	186.1	0.983	0.995	1.004	0.970	1.030	1.020	0.996	1.041	0.955
Pb-212	238.63	0.980	0.993	1.006	0.971	1.029	1.021	0.997	1.042	0.955
Pb-214	241.91	0.980	0.992	1.007	0.971	1.029	1.021	0.997	1.042	0.954
Pb-214	295.2	0.979	0.991	1.008	0.972	1.028	1.021	0.997	1.042	0.954
Ac-228	338.322	0.978	0.990	1.009	0.973	1.027	1.021	0.997	1.043	0.953
Pb-214	351.4	0.978	0.990	1.009	0.973	1.027	1.022	0.997	1.043	0.953
Tl-208	510.8	0.977	0.989	1.010	0.974	1.026	1.022	0.998	1.044	0.952
Tl-208	582.7	0.977	0.988	1.011	0.975	1.026	1.022	0.998	1.044	0.952
Bi-214	609.312	0.977	0.988	1.011	0.975	1.025	1.022	0.998	1.044	0.952
Cs-137	661.66	0.976	0.988	1.011	0.975	1.025	1.022	0.998	1.044	0.952
Bi-212	727.264	0.976	0.987	1.011	0.975	1.025	1.022	0.998	1.044	0.951
Ac-228	910.8	0.976	0.987	1.012	0.976	1.024	1.023	0.998	1.045	0.951
Ac-228	964.64	0.976	0.987	1.012	0.976	1.024	1.023	0.998	1.045	0.951
Ac-228	968.971	0.976	0.987	1.012	0.976	1.024	1.023	0.998	1.045	0.951
Bi-214	1120.4	0.975	0.986	1.013	0.976	1.024	1.023	0.998	1.045	0.950
K-40	1460.83	0.975	0.986	1.013	0.977	1.023	1.023	0.998	1.046	0.950

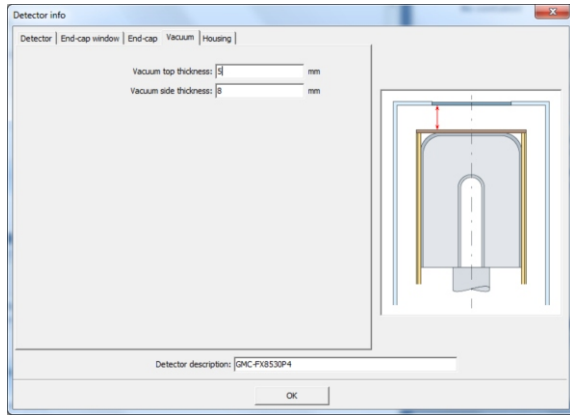


Figure 6. Experimental set-up of detector vacuum top thickness in ANGLE with red arrow showing true value of 5 mm

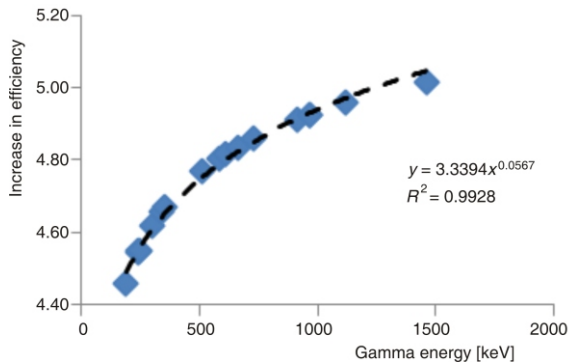


Figure 7. Percentage increase in absolute efficiency due to error introduced in the vacuum top thickness; true value = 5 mm, error value = 3 mm, key = Vtt – 2 mm. Efficiency increase range: 4.46 to 5.02 %

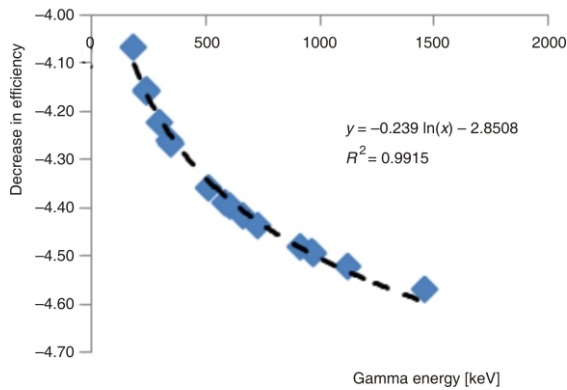


Figure 8. Percentage increase in absolute efficiency due to error introduced in the vacuum top thickness, true value = 5 mm, error value = 7 mm, key = vtt + 2 mm. Efficiency decrease range: -4.07 to -4.57 %

rors are modeled in figs. 7 and 8 and show that the maximum impact occurred at the higher energies. Equation (11) depicts the variation of Y for understating the vacuum top thickness and eq. 12 for overstating the same parameter

$$y = 3.3394x^{0.0567} \tag{11}$$

For fig. 7, the radioactivity values at the lower end of the spectrum (186 keV) will be reduced by 4.46% and at the higher end (1460 keV) by 5.02% based on eq. (11) when a -40% error is made in the vacuum top thickness.

In fig. 8, overstating the vacuum top thickness by 2 mm, in relation to a true value of 5 mm, results in the efficiency erroneously decreasing logarithmically by the expression shown in eq. (12)

$$y = 0.239 \ln(x) - 2.8508 \tag{12}$$

From fig. 8, the radioactivity values at the lower end of the spectrum (186 keV) were increased by 4.07% and at the higher end (1460 keV) by 4.6% based on eq. (12) when a +40% error is made in the vacuum top thickness.

Discussion for detector vacuum error modeling

The major reasons for the vacuum layer above the detector are to: (a) insulate the crystal from the outer layer temperature of the detector housing, (b) reduce any vibrations that may generate a frequency (microphonics) that would add noise to the system, (c) provide some distance from the outer end cap which is at ground potential since the outside of the detector is typically at the bias voltage potential, and (e) ensure that contaminants from the air are not attracted to the surface of the cold crystal, resulting in a negative effect on the charge collection characteristics (of the crystal) [31]. The results of these modeled errors are expected and easily explainable by the physical processes that occur in gamma spectroscopy using semiconductors. Reduction in the distance travelled by the gamma from the source to the active volume is reduced if the vacuum level between the crystal and the end-cap window is reduced. This reduction would allow more gammas to arrive and interact inside the active volume due to an increase in solid angle. Since a linear relationship exists between the efficiency and the solid angle, the efficiency of the detector is increased. The opposite effect would occur when the vacuum distance on top of the crystal is increased. Not surprisingly, the error in the vacuum side thickness is negligible for this geometry, as most gammas would enter the detector from the top. The gammas entering the side of the crystal would be mainly X-rays from interaction in the surrounding lead shield. We anticipate that the side thickness would have a more significant impact, if Marinelli containers were used or if the source radius was much greater than the crystal radius.

Modeling of error in detector crystal geometry – radius and height

In this section we introduced two error scenarios into the efficiency calculation by changing the detector crystal radius value of 42.5 mm to 40.5 mm, and 44.5 mm. The resulting efficiency curves from these two scenarios were compared with the actual efficiency curve, and the average percentage value of the changes noted.

Figures 10 and 11 show how error introduced in measurement of the crystal radius impacts the absolute efficiency values. In figure 10 understating the detector crystal radius by 2 mm, results in an average decline of 2.6% with the impact maximized at the lower energies and modeled by the expression shown in eq. (13)

$$Y = 5E-07x^2 - 0.0012x + 3.116 \quad (13)$$

Figure 11 shows the modeling of overstating the crystal radius by 2 mm by the expression in eq. (14)

$$Y = 0.308 \ln(x) - 4.5464 \quad (14)$$

Figures 13 and 14 and eqs. (13) and (14), show how error introduced in the detector crystal height is modeled in ANGLE. As shown in tab. 2, we introduce

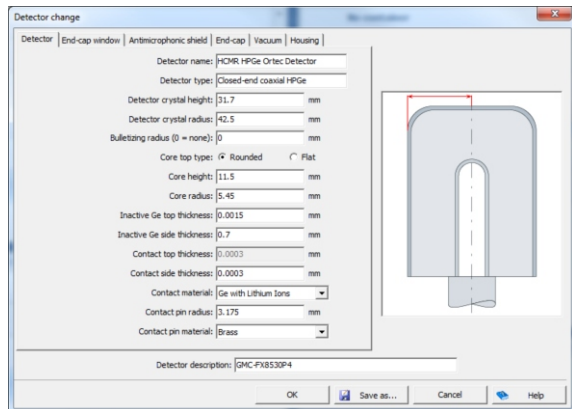


Figure 9. Detector crystal radius in ANGLE with arrow depicting parameter value of 42 mm

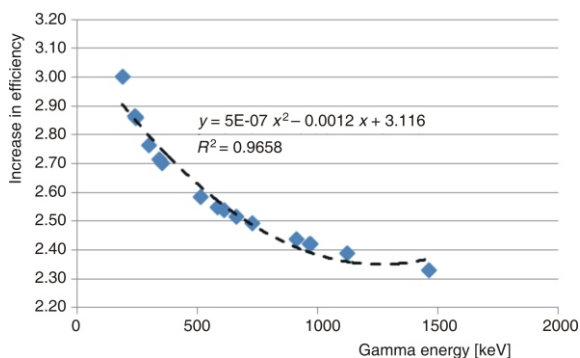


Figure 10. Error in detector crystal radius, true value = 42.5 mm, error value = 40.5 mm, radius under measured by 2 mm. Efficiency increase range: 2.33 to 3.00%

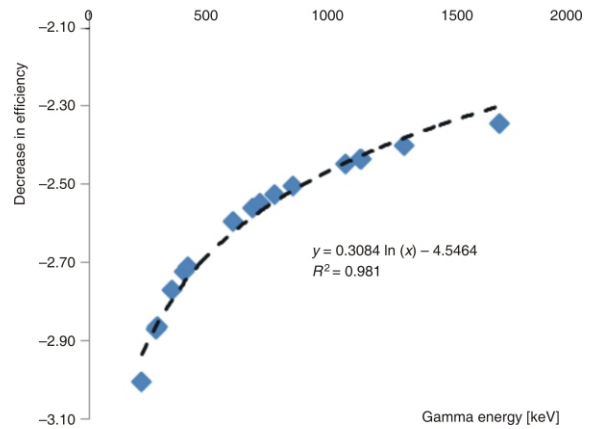


Figure 11. Error in detector crystal radius, true value = 42.5 mm, error value = 44.5 mm, radius over measured by 2 mm. Efficiency decrease range: -3.00 to -2.34 %

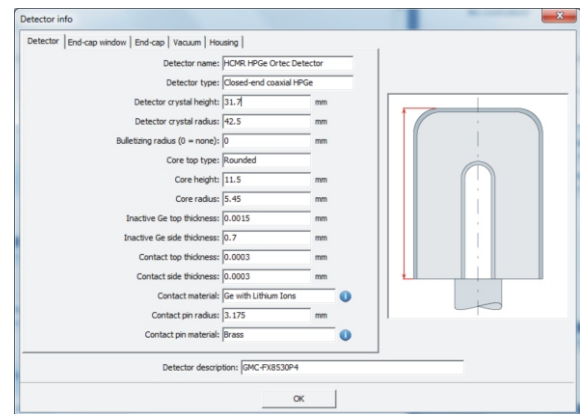


Figure 12. Detector crystal height in ANGLE with arrow depicting parameter value of 31.7 mm

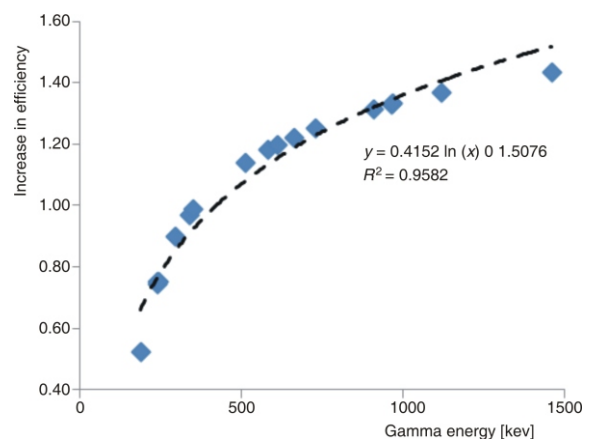


Figure 13. Error in detector crystal height, true value = 31.7 mm, error value = 29.7 mm, height under measured by 2 mm. Efficiency increase range: 0.52 to 1.43%

a six percent error in the height of the crystal and report on the percentage variation of the new efficiency curve from the correct value.

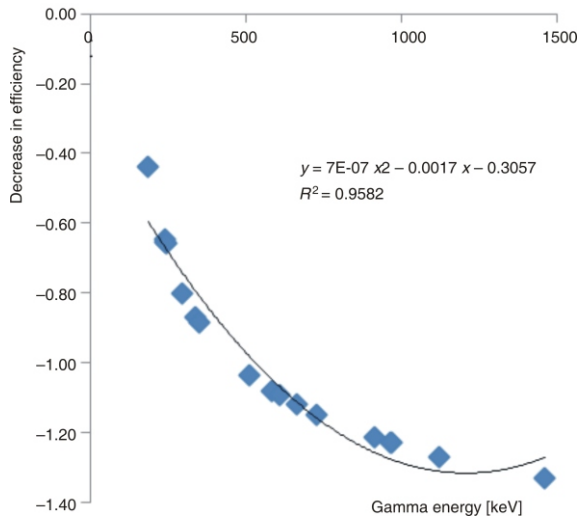


Figure 14. Error in detector crystal height, true value = 31.7 mm, error value = 33.7 mm, height over measured by 2 mm. Efficiency decrease range: -0.44 to -1.33%

The percentage variation in fig. 13 is described by the expression in eq. (15)

$$Y = 0.4152 \ln(x) - 1.5076 \quad (15)$$

The percentage variation in fig. 14 is described by the expression in eq. (16)

$$Y = 7E-07x^2 - 0.0017x - 0.3057 \quad (16)$$

Discussion on crystal size error modeling

We note that error in crystal height and radius that resulted in a crystal size larger than its true value (figs. 10 and 13), resulted in an increase in efficiency over the true value. This increase in efficiency can be explained due to an increase in the solid angle subtended on the crystal face when the crystal diameter increases. In the case of a crystal with greater height, the active volume for which gamma interaction, mainly by Compton scattering, photoelectric effect and pair-production occurs increases, hence more gammas will be recorded leading to an increase in absolute efficiency. We present a number of theoretical and empirical results that validate our expectations. The first shown in eq. (17), is that there is a direct relationship between the relative efficiency ϵ_{rel} (%) and the active volume; the efficiency increases faster with detector radius than detector length. This is an approximate and not dimensionally correct relationship [32]

$$\text{Relative efficiency } \epsilon_{rel}[\%] = \text{Volume}/4.3 \quad (17)$$

This relative photopeak efficiency which is defined as the 1.332 keV peak of a Co-60 point source 25 cm centered on the end -cap of a detector. This efficiency number is part of the standard for Ge detectors,

and is relative to a perfect 3" diameter by 3" deep right circular cylinder of NaI(Tl) with the same geometry to the source. Since this is the response to about a 1.3 MeV gamma, the volume alone is not the only factor when determining the relative photopeak efficiency. The dimensions can vary with any specific Ge detector since these are individually grown crystals. For example a longer cylindrical shape can require a different total volume than a large diameter crystal with less depth. There is more to this calculation than simply the total volume. Using the factor 1/4.3 is a way to roughly calculate the relative photopeak efficiency [33].

Our research confirms (as shown in tab. 2, and comparing values for dcr-2mm and dch-2mm in fig. 5) that the detector crystal radius has a greater impact on efficiency than crystal height; the normalized sensitivity value for the detector radius is greater than that of the detector height by a factor of 5.

Another empirical formula describing the relationship between the relative efficiency (%) and the active volume is shown in eq. (18) and indicates a more detailed requirement on the detector diameter [34]. The diameter factor we developed in eq. (13) bears some similarity to the diameter factor in eq. (18)

$$\text{Relative efficiency } \epsilon_{real} = KD^\alpha L^\beta \quad (18)$$

where D is the active crystal diameter in decimeters, L – the crystal length in decimeters, $K = 2.4321$, $\alpha = 2.8155$, and $\beta = 0.7785$ [32].

For planar detectors, the Mowatt formula has been proposed and found to give efficiency results with an accuracy of 1.5% in the energy range of 100 keV-1400 keV [35]. This expression also expresses a direct relationship between the efficiency and the detector size in the a_5 factor

$$\epsilon = \frac{a_1 F' \exp(-\mu_{Ge} a_2) \tau \alpha a_3 \exp(-a_4 E)}{\tau \alpha [1 - \exp(-\mu_{Ge} a_5)]} \quad (19)$$

where $F' = \prod_i \exp(-\mu_i x_i)$ and is the product of the attenuation factors outside the intrinsic area, τ is the photoelectric absorption coefficient in germanium at energy E , α – the Compton absorption coefficient at energy E , a_2 – the thickness of the germanium front dead layer, and a_5 – the effective detector depth

The Freeman-Jenkins equation has also been reported to give a 1% accuracy over the 500 keV-1500 keV range for the relative efficiency of cylindrical and trapezoidal detector and is denoted as

$$\epsilon = 1 - \exp(-\tau x) - \sigma A \exp(-BE) \quad (20)$$

where τ is the photoelectric constant, x – the thickness of the detector, and σ – the Compton coefficient, and A and B are constants to be determined from measurements.

Modeling of error in bulletizing radius

In this section we introduce an error scenario into the efficiency calculation by introducing a detector bulletizing radius of 8 mm where there should be none. The resulting efficiency curve from this scenario was compared with the actual efficiency curve, and the average percentage value of the changes noted.

Figure 16 shows how error in the bulletizing radius was modeled resulting in an average increase of 2.24% in the absolute efficiency values over the range 180 keV to 1500 keV, the greater percentage increases occurring at the higher energies. The impact is modeled in eq. 21

$$y = 1E-06x^2 + 0.0021x + 1.15148 \quad (21)$$

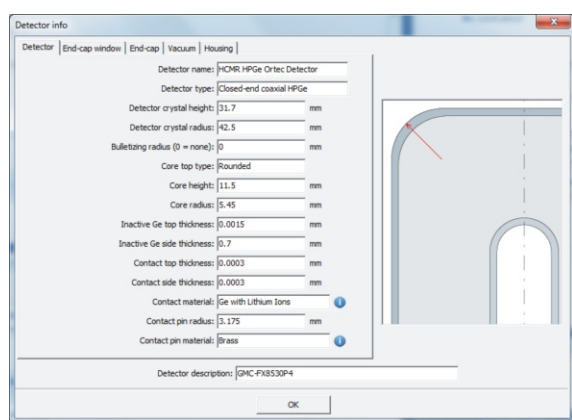


Figure 15. Detector bulletizing radius in ANGLE with depiction with arrow

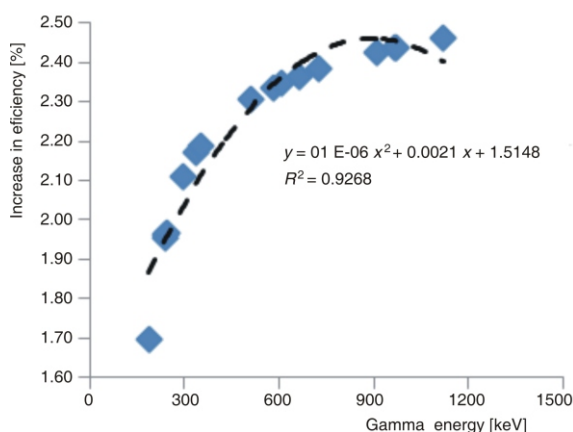


Figure 16. Error in introducing a bulletizing radius: true value = 0 mm, error value = 8 mm

Discussion on error in bulletizing radius

Our results, as shown in eq. (21), show a quadratic dependence on the over-reporting of absolute efficiency, when a bulletizing radius of 8 mm is incor-

rectly assumed with respect to the correct no-bulletizing results. In our investigation, the minimum error (1.7%) occurred at the lowest energy and the maximum (2.5%) at the highest energy for the counting geometry investigated. Mihaljević *et al* also showed a quadratic relationship between the errors and bulletizing radius with the smaller gammas having the greater effect [14].

CONCLUSIONS

When measuring the solid angle or absolute efficiency of a detector using absolute or semi-empirical calculations, incorrect engineering details about the detector construction will result in the introduction of systematic errors. A typical HPGe detector set-up for the measurement of full peak efficiency using ANGLE may be characterized by as much as 64 specifications distributed as shown in brackets across the crystal (15), end-cap window (3), end-cap (4), vacuum (2), housing (8), source container (9), source geometry (8), intercepting layers, gamma energies (1 set), reference efficiency curve (13), and the calculation precision. In this paper, we restricted our investigations to the 32 parameters that characterized the detector and demonstrated that errors related to the vacuum layer above the detector crystal, the bulletizing specification of the crystal, and the crystal size, had the most impact on the efficiency value for a detector setup for the spectrometric analysis of soil in a cylindrical container and in contact geometry with the detector. The impact of these uncertainties, characterized as the percentage deviation with respect to the correct absolute efficiency curve, was found to be dependent on whether the error values were above or below the correct values that characterized the detector. In all cases the impacts were found to vary either quadratically or logarithmically over the energy range of 180 keV to 1500 keV. A number of other parameters shown in tab. 2 were determined to have a very small impact when their errors were modeled; these parameters had their NSI rounded to 0.00. In this paper, we modeled these detector errors mathematically for the first time, allowing spectrometrists using this counting geometry and semi-empirical efficiency calculation method to make error corrections to their gamma activity values done with detector characterizations that were incorrect. Since full peak efficiency calculation, using ANGLE's efficiency transfer method reduces error propagation due to partial error compensation in the $\bar{\Omega} / \bar{\Omega}_{ref}$ factor in eq. (3), ANGLE is generally considered as a good tool for handling efficiency calculations [14]. Finally, this research does the following for the typical counting geometry employing p-type HPGe detectors for soil and sediment radionuclide analysis; (a) introduces the normalized sensitivity impact parameter (NSI) which allows a comparative analysis to be made of the impact of detector specification uncertainties, (b) proposes a default set of detector characterization val-

ues that may be used in semi-empirical methods for generating a reference efficiency curve using the efficiency transfer method inherent in ANGLE software (a notation is inserted that these values are to be used with the understanding that their uncertainty impact on the full-peak efficiency, though not very significant in this counting arrangement, is not non-zero), and (c) develops an understanding through mathematical modeling, of how uncertainties in the most important detector specifications affect the full-energy peak efficiency value in the gamma range of 180 keV-1500 keV.

Application of research results

The results shown in this paper may be incorporated into further releases of ANGLE to reduce the effects of systematic errors and/or produce results with a margin of error associated with common user input errors. Also in future releases of ANGLE, the default values presented in this paper may be incorporated as initial default values for specific radiometric application and the parameters with higher error impact highlighted. The correction factors listed in this study should be useful in making corrections to activity results to accommodate any uncertainty. We recommend additional studies to include a wider variety of detectors, detector parameters and counting geometries to ascertain how the errors in their engineering specification propagates.

ACKNOWLEDGEMENTS

We acknowledge the following persons and institution for their kind assistance that resulted in the completion of this research paper: Slobodan Jovanovic and Aleksandar Dlabac, University of Montenegro, Podgorica, Montenegro.

AUTHOR CONTRIBUTIONS

Theoretical analysis was carried out by M. Miller and M. Voutchkov and experiments were carried out by M. Miller. Both authors analyzed and discussed the results. The manuscript was written by M. Miller.

REFERENCES

- [1] Wright, A. G., Absolute Calibration of Photomultiplier Based Detectors – Difficulties and Uncertainties, *Nuclear Instruments and Methods in Physics Research Section A: Accelerators, Spectrometers, Detectors and Associated Equipment*, 433 (1999), 1-2, pp. 507-512
- [2] Peelle, R. W., Spencer, R. R., Counting Anticoincidences to Reduce Statistical Uncertainty in the Calibration of a

- Multiplicity Detector, *Nuclear Instruments and Methods in Physics Research*, 211 (1983), 1, pp. 167-170
- [3] Simpson, B. R. S., Dead time Measurement and Associated Statistical Uncertainty by Means of a Two-Detector Paired-Source Method, *International Journal of Radiation Applications and Instrumentation, Part A. Applied Radiation and Isotopes*, 42 (1991), 9, pp. 811-814
- [4] Gasparro, J., et al., The Effect of Uncertainties in Nuclear Decay Data on Coincidence Summing Calculations for Gamma-Ray Spectrometry, *Czechoslovak Journal of Physics*, 56 (2006), 1, pp. D203-D210
- [5] Piesch, E., Burgkhardt, B., Sauer, D., Electrochemical Etching of CR-39 and Makrofol De Track Detectors: Investigation of Parameters Affecting the Overall Uncertainty of Measurement, *International Journal of Radiation Applications and Instrumentation, Part D. Nuclear Tracks and Radiation Measurements*, 19 (1991), 1-4, pp. 211-214
- [6] Eappen, K. P., et al., Estimation of Radon Progeny Equilibrium Factors and Their Uncertainty Bounds Using Solid State Nuclear Track Detectors, *Radiation Measurements*, 41 (2006), 3, pp. 342-348
- [7] Whitlow, H. J., et al., Measurement and Uncertainties of Energy Loss in Silicon over a Wide Z1 Range Using Time of Flight Detector Telescopes, *Nuclear Instruments and Methods in Physics Research Section B: Beam Interactions with Materials and Atoms*, 195 (2002), 1-2, pp. 133-146
- [8] Bonifazi, C., Letessier-Selvon, A., Santos, E. M., A Model for the Time Uncertainty Measurements in the Auger Surface Detector Array, *Astroparticle Physics*, 28 (2008), 6, pp. 523-528
- [9] Shishkina, E. A., Performance Parameters and Uncertainty of the Method for Assessment of ⁹⁰Sr Concentration in Small Powder Samples Using α -Al₂O₃:C Beta Detectors, *Radiation Measurements*, 47 (2012), 1, pp. 19-26
- [10] Fromm, M., et al., Principle of Light Ions Micromapping and Dosimetry Using a CR-39 Polymeric Detector: Modelized and experimental uncertainties, *Nuclear Tracks and Radiation Measurements*, 21 (1993), 3, pp. 357-365
- [11] Stepan, R., et al., Uncertainties of Gas Chromatographic Measurement of Troublesome Pesticide Residues in Apples Employing Conventional and Mass Spectrometric Detectors, *Analytica Chimica Acta*, 520 (2004), 1-2, pp. 245-255
- [12] Slaninka, A., Slavik, O., Necas, V., Uncertainty Analysis of In-situ Gamma Spectrometry Measurements of air Cleaning Filter Cartridges and 200 L Drums by a HPGe Detector, *Applied Radiation and Isotopes*, 68 (2010), 7-8, pp. 1273-1277
- [13] Kastanya, D., The Importance of Uncertainties in the ROP Detector Layout Design Process for CANDU Reactors, *Annals of Nuclear Energy*, 38 (2011), 4, pp. 775-780
- [14] Mihaljević, N., Dlabac, A., Jovanović, S., Accounting for Detector Crystal Edge Rounding in Gamma Efficiency Calculations – Theoretical Elaboration and Application in ANGLE Software, *Nucl Technol Radiat*, 27 (2012), 1, pp. 1-12
- [15] Gilmore, G. R., Practical Gamma-Ray Spectrometry, 2nd ed, John Wiley & Sons, Ltd., West Sussex, UK, 2008, p. 389
- [16] ***, Princeton Gamma-Tech, *Nuclear Products Catalog*, 2012
- [17] Jovanović, S., et al., ANGLE: A PC-Code for Semiconductor Detector Efficiency Calculations, *Journal of Radioanalytical and Nuclear Chemistry*, 218 (1997), 1, pp. 13-20

- [18] Abbas, K., *et al.*, Reliability of Two Calculation Codes for Efficiency Calibrations of HPGe Detectors, *Applied Radiation and Isotopes*, 56 (2002), pp. 703-709
- [19] Moens, L., *et al.*, Calculation of the Absolute Peak Efficiency of Gamma-Ray Detectors for Different Counting Geometries, *Nuclear Instruments and Methods in Physics Research*, 187 (1981), 2-3, pp. 451-472
- [20] Mihaljević, N., *et al.*, "EXTSANGLE" – An Extension of the Efficiency Conversion Program "SOLANG" to Sources with a Diameter Larger than that of the Ge-Detector, *Journal of Radioanalytical and Nuclear Chemistry*, 169 (1993), 1, pp. 209-218
- [21] De Corte, F., *et al.*, Introduction of Marinelli Effective Solid Angles for Correcting the Calibration of NaI(Tl) Field Gamma-Ray Spectrometry in TL/OSL Dating, *Journal of Radioanalytical and Nuclear Chemistry*, 257 (2003), 3, pp. 551-555
- [22] Byun, S. H., *et al.*, Efficiency Calibration and Coincidence Summing Correction for a 4 NaI(Tl) Detector array, *Nucl. Instrum. and Methods in Phys. Res., Section A: Accelerators, Spectrometers, Detectors and Associated Equipment*, 535 (2004), 3, pp. 674-685
- [23] Vukotić, P., *et al.*, On the Applicability of the Effective Solid Angle Concept in Activity Determination of Large Cylindrical Sources, *Journal of Radioanalytical and Nuclear Chemistry*, 218 (1997), 1, pp. 21-26
- [24] Vidmar, T., *et al.*, Testing Efficiency Transfer Codes for Equivalence, *Applied Radiation and Isotopes*, 68 (2010), 2, pp. 355-359
- [25] ***, Ortec, Advanced Efficiency Calibration Software for High Purity Germanium Gamma-Ray Detectors, 2012, Retrieved from <http://old.ortec-online.com/software/angle.htm>
- [26] Mihaljević, N., Dlabac, A., Jovanović, S., Accounting for Detector Crystal Edge Rounding in Gamma Efficiency Calculations – Theoretical Elaboration and Application in ANGLE Software, *Nucl Technol Radiat*, 27 (2012), 1, pp. 1-12
- [27] Knoll, G. F., Radiation Detection and Measurement, 4th ed, John Wiley and Sons, New York, 2009, pp. 335-338
- [28] ***, Canberra, Model 8715 Analog-to-Digital Converter, 2012, Retrieved from http://www.canberra.com/products/radiochemistry_lab/nim-analog-digital-converter.asp.
- [29] Tsabaris, C., *et al.*, Radioactivity Levels of Recent Sediments in the Butrint Lagoon and the Adjacent Coast of Albania, *Applied Radiation and Isotopes*, 65 (2007), 4, pp. 445-453
- [30] ***, Ortec, Advanced Efficiency Calibration Software for High Purity Germanium Gamma-Ray Detectors, 2012, Available from <http://old.ortec-online.com/software/angle.htm>
- [31] Kennedy, B., Personal discussion on vacuum layer above detector crystal, 2012
- [32] ***, Ortec, Overview of Semiconductor Photon Detectors. 2012
- [33] Kennedy, B., Clarification on Relative Efficiency, Personal Communication, 2012
- [34] Khoo, T. L., Relative Efficiency of Detector, 2012
- [35] Tsoulfanidis, N., Measurement and Detection of Radiation, 2nd ed, Taylor & Francis, Washington D. C, 1995, p. 636

Received on October 15, 2012

Accepted on March 25, 2013

Морис МИЛЕР, Митко ВУЧКОВ

МОДЕЛОВАЊЕ УТИЦАЈА НЕСИГУРНОСТИ ПАРАМЕТАРА ЕФИКАСНОСТИ HPGe ДЕТЕКТОРА УПОТРЕБОМ ПРОГРАМА ANGLE

Циљ овог рада је да се моделује утицај несигурности у инжењерским спецификацијама за вредности параметара ефикасности типичног HPGe детектора п-типа, при мерењу узорака земљишта у геометрији у којој је узорак у контакту са детектором. Уведен је параметар "нормализован утицај осетљивости" који омогућава компаративну анализу утицаја несигурности из спецификација детектора и формирање табеле корекционих фактора за најважније параметре. Области детектора за које је утврђено да су најподложније грешци су геометрија кристала, вакуумски слој изнад кристала и радијус заобљења кристала. По први пут су главни утицаји математички моделовани и утврђено је да се понашају као квадратна или логаритамска функција у опсегу енергија од 180 keV до 1500 keV. Предложен је скуп карактеристичних вредности за детектор које се могу користити у програму ANGLE за генерисање референтне криве ефикасности употребом методе трансфера ефикасности, која је део програмског пакета. Ове вредности треба користити имајући на уму да утицај њихове несигурности на максималну ефикасност, иако не превише битан у овом облику бројања, нема нулту вредност.

Кључне речи: карактеризација детектора, програм ANGLE, несигурности, HPGe детектор, ефикасности детектора